Carrier Multiplication in Semiconductor Nanocrystals: Theoretical Screening of Candidate Materials Based on Band-Structure EffectsC[(Jun-Weits)]TJ1Luo,ts

$$N_{eh}^{max}(\hbar\omega) = [\hbar\omega/\varepsilon_g^{dot}] \quad (2)$$

where the square bracket denotes the integer part of $\hbar\omega/\varepsilon_g^{dot}$. If we extract E_{th} and λ_{CM} from the energy-conservation function of eq 2 by taking the lower edge of each step, we obtain the simple expectation that $E_{th} = 2\varepsilon_g^{dot}$ and $\lambda_{CM} = 1/\varepsilon_g^{dot}$.

Experimentally,[10,12,16,17] the DCM energy threshold E_{th} and the DCM coefficient λ_{CM} were found to be material dependent, but for a given material to be nearly independent of the nanocrystal band gap ε_g^{dot}, or, equivalently, of the nanocrystal size. Table 1 summarizes the values of the scaled quantities $E_{th}/\varepsilon_g^{dot}$ and $\lambda_{CM}\varepsilon_g^{dot}$ obtained from experiment. Surprisingly, the experimentally determined values of λ_{CM} for PbSe, PbS, CdSe, and Si (Table 1) are larger than those predicted by the energy-conservation rule (eq 2), although the condition $N_{eh}(\hbar\omega) < N_{eh}^{max}(\hbar\omega)$ is satisfied by virtue of the relatively large values of E_{th}. The coefficients E_{th} and λ_{CM} of eq 1 provide a measure of the efficiency of the DCM process in different semiconductor nanocrystals. Recent experiments have questioned the existence of DCM in CdSe[18] and InAs[19] nanocrystals. Tuan Trinh et al.[20] recently confirmed the occurrence of DCM in PbSe nanocrystals, although with much lower efficiency than previously reported.[10,12]

We wish to isolate in this work bulk band structure effects from surface effects. Thus, we will model here the electronic levels of the dot by an approach that eliminates surface effects. The questions we wish to address are as follows: (i) Is the lack of translational symmetry in nanocrystals the reason for high carrier-multiplication efficiency and is strong quantum confinement necessary for efficient carrier multiplication? (ii) Competing processes: Can impact ionization outperform the inverse process of Auger recombination (Figure 1c), thereby creating a net carrier multiplication effect? Can DCM be faster than competing decay processes, such as phonon-assisted relaxation? (iii) Which property of

functional of the single-particle density of states $\rho(\varepsilon)$, so a correct determination of $\rho(\varepsilon)$ is crucial to accurately determine $R_2(E)$. As shown by eqs 6 and 7, the calculation of $R_2(E)$ may require a very large number of nanocrystal energy levels ε_n, if the multiexciton energy E is large. Thus, a direct calculation of $R_2(E)$ using first-principles methods or atomistic semiempirical methods (such as tight-binding or pseudopotential) would be costly. Here we want to calculate $R_2(E)$ for several nanocrystal materials and nanocrystal sizes. So we resort to an approximation for calculating the nanocrystal energy levels.

Although DCM can be affected by both quantum-confinement effects (reflecting the underlying electronic structure of the confined dot-interior states) and surface special effects, we are interested in isolating the former.

To do so, we use here the truncated-crystal approximation (TCA) to calculate the single-particle DOS (eq 5), the single-exciton and biexciton densities of states (eqs 6 and 7), and the DCM "figure of merit" $R_2(E)$ (eq 4). The idea behind the TCA[24−28] is to obtain the single-particle energy levels of a *nanocr stal* (containing many atoms) from the energy bands of the corresponding *b.ılk material* (containing only a few atoms per cell), calculated at special $\bar{}$ points in the bulk Brillouin zone, such that the envelope function $F(\ )\ = \sum^{-} e^{i\bar{}\cdot\ }$ vanishes at the surface of the nanocrystal (Figure 2). This approach was used over 30 years ago to predict the energy levels of finite graphene strips from the band structure of (infinite periodic) graphite or boron nitride[24,25] and to approximate the levels of finite slabs of Si from the Si bulk band structure.[26,28] The TCA approach was later refined and improved[27] to include the effects of a finite potential barrier. While this does bring about an improvement, we judge that in the present survey of many materials the trends are not affected much by this correction. Indeed, the valence-band and conduction-band offsets between semiconductors and its the surrounding organic molecules are large in colloidal nanostructures,[29] and the effective mass discontinuity at the dot surface further enhances the electronic states localization.[30] Consequently, for a rapid screening of materials, we will use the infinite-barrier TCA described above instead of the finite-barrier TCA.[27] Also note that the TCA includes multiple band edge valleys (e.g., Γ, *X*, and *L*) but not their coupling. The inclusion of the effect of higher valleys on the density of states has been shown[27] to be important.

In the TCA the DOS of a nanocrystal is given by

$$\rho^{\mathrm{TCA}}(\varepsilon) = \sum_{n=1}^{N_{\mathrm{bands}}} \sum_{\bar{}} \delta(\varepsilon - \varepsilon_{n,\bar{}}^{\mathrm{bulk}}) \tag{11}$$

where $\varepsilon_{n,\bar{}}^{\mathrm{bulk}}$ is the energy of the bulk band n calculated at the special TCA point $\bar{}$ (Figure 2). In this work we consider cubic nanocrystals, a choice that simplifies the use of the TCA, compared to other nanocrystal shapes. As shown in Figure 2 for a cubic nanocrystal of edge L, the set of special $\bar{}$ points is given by

$$\bar{}_{i,j,k} = \ _0 + \frac{\pi}{L}(i, j, k) \tag{12}$$

that are located inside the bulk Brillouin zone. Here $_0$ is the point of the band edge (CBM or VBM) and i, j, k are positive intefor

interaction) underestimates the band gap by ≈60% and the conduction band effective mass by ≈40%. The approach followed here is to shift the LDA conduction band up to correct for the band gap error. However, this does not solve the entire problem because the LDA effective masses are still incorrect. As a result, the LDA band gap (Figure 3a) and DOS (Figure 3b) are systematically shifted relative to EPM. Furthermore, the LDA-predicted band gaps of narrow-gap semiconductors (e.g., InAs, InSb, GaSb, and Ge) are negative, so the band-edge states are spuriously coupled. This significantly complicates the use of LDA within the TCA approximation. Therefore, in the following we will use EPM/TCA rather than C-LDA/TCA. The EPM calculated single-particle density of states as obtained from TCA is given in Figure 4 for a few materials and a few sizes.

I . ' t . **.** Figure 5 shows the experimentally determined band gaps of 27 III−V,

a function of the nanocrystal band gap ε_g^{dot} showing three sizes for each dot. There is an overall linear increase of E_0 with the band gap, which is evident from Figure 10a. To remove this linear background, in Figure 10b, we show E_0/ε_g^{dot} as a function of the band gap ε_g^{dot}. We see from Figure 10b that PbSe, Si, GaAs, CdSe, and InP nanocrystals have a significantly lower DCM critical energy than GaSb, InSb, Ge, and InAs nanocrystals. Figure 10a shows that as the dot size increases, E_0 decreases, so larger dots are better than smaller dots. Figure 10b shows that the *normali ed* E_0/ε_g^{dot} sometimes increases (e.g., Si) and sometimes decreases (e.g., InAs) as the dot size increases.

The application of nanocrystals as light absorber in solar-cell devices requires a good match of the nanocrystal absorption spectrum with the solar spectrum.[40] Using a detailed balance model, Hanna and Nozik[41] found that, in the presence of carrier multiplication, the optimal value of the nanocrystal band gap is around 0.7−0.9 eV. We find that PbSe nanocrystals, having sufficiently small band gaps and sufficiently low DCM threshold, are the best candidates for DCM-based solar-cell applications. Although Si has low DCM critical energy and large DCM figure of merit, its absorption spectrum for small nanocrystal size does not match the solar spectrum.[40]

. . The DCM process involves the creation of two or more electron−hole pairs as a result of exciting a

. Calculated TCA band gap of nanocrystals as a function of effective radius for the semiconductors GaAs, GaSb, InAs, InP, InSb, Si, Ge, and PbSe. Vertical red arrows indicate direct−indirect electronic phase transitions.

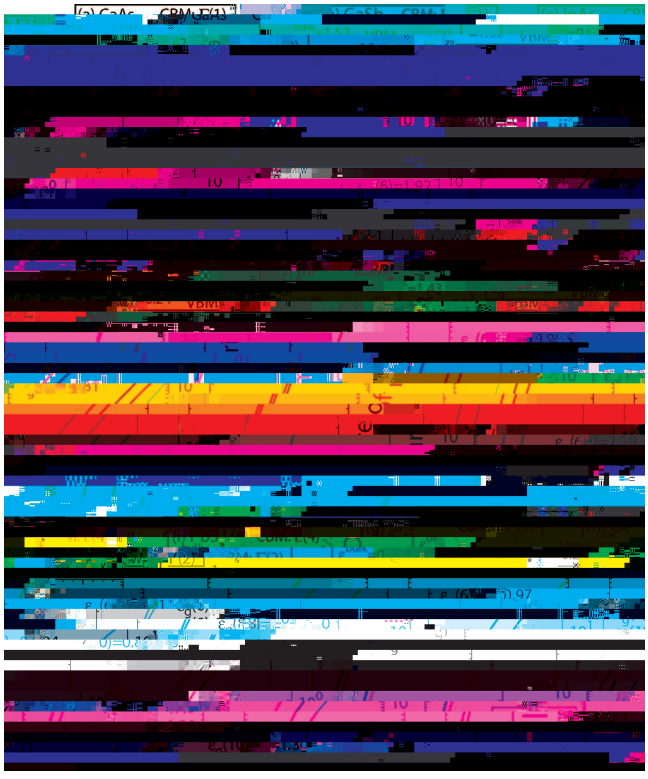

. The DCM figure of merit R_2 (eq 4) of cubic nanocrystals of size $(N \times N \times N)a_0$ for $N = 6$ (green), $N = 8$ (blue), and $N = 10$ (red) for different semiconductors as a function of the reduced photon energy. The insets give the nanocrystal band gap (in eV).

. The DCM figure of merit $R_2(E)$ at photon energy $E = 2.6\varepsilon_g^{dot}$ for different nanocrystals of size $N = 6$.

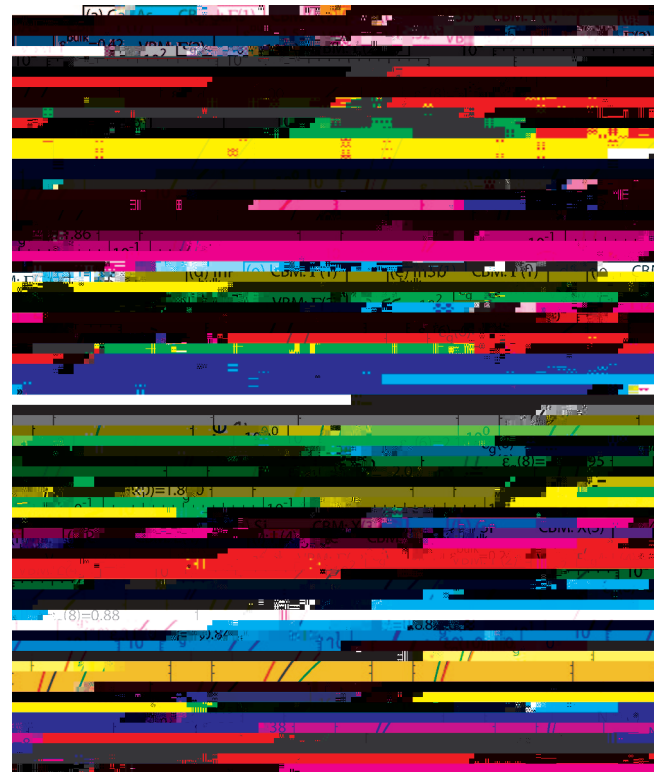

. Same as Figure 7 but using the figure of merit R_1 of eq 3, which does not consider the Coulomb selection rule.

(i) The degeneracy of the CBM and VBM is the most important factor for DCM efficiency. Not including spin degeneracy, the conduction-band is nondegenerate at Γ, 3-fold-degenerate at *X*, and 4-fold-degenerate at the *L*-point. PbSe (Figure 7i), for which both the CBM and VBM are located at the *L*-point, has the highest DCM figure of merit among the semiconductors calculated here.

(ii) The energy spacing between the Γ-, *X*-, and *L*-valleys is also important for direct Γ−Γ semiconductors. Although the CBM state of *bulk* GaAs (Figure 7a), InSb (Figure 7e) and GaSb (Figure 7b) is Γ-derived, the electron states of the corresponding small *nanocrystals* derive from the 4-fold *L*-point Bloch state, because in these materials there is an electronic Γ-to-*L* transition (Figure 6) due to the small Γ−*L* valley-spacing in the bulk (Figure 5). Notably, from this point of view InAs is worse for DCM because there is no Γ-to-*L* transition at any nanocrystal size on account of the very large Γ−*L* spacing in bulk InAs (Figure 5).

(iii) Relative to properties (i) and (ii), the importance of the effective masses for the DCM process is small.

We see from Figure 7 that for all nanocrystal materials and sizes, $R_2(E)$ increases monotonically with energy E. The "steepness" of the figure of merit $R_2(E)$ correlates well with the experimentally measured values of λ_{CM} (see Table 1). For example, we find that Si and PbSe nanocrystals, which have a large λ_{CM}, also have a large $R_2(E)$, while InAs nanocrystals, which have a small λ_{CM}, also have a rather flat $R_2(E)$. Larger values of $R_2(E)$ indicate larger DCM efficiency.

Interestingly, by considering band structure effects we find that as the dot size increases the DCM critical energy E_0 (the photon energy at which $R_2(E)$ becomes ≥ 1) is reduced, suggesting improved DCM. However, whether the normalized E_0/ε_g increases or decreases as the dot size increases depends on dot material.

t. This work was funded by the U.S. Department of Energy, Office of Science, Basic Energy Science, Materials Sciences and Engineering, under Contract No. DE-AC36-99GO10337 to NREL.

(1) Shockley, W.; Queisser, H. J. *J. Appl. Ph s.* **1 1**, *32*, 510.
(2) Nozik, A. J. *Ph sica E* **2002**, *14*, 115.
(3) Kolodinski, S.; Werner, J. H.; Wittchen, T.; Queisser, H. J. *Appl. Ph s. Lett.* **1 3**, *63*, 2405.
(4) Geist, J.; Gardner, J. L.; Wilkinson, F. J. *Ph s. Rev. B* **1 0**, *42*, 1262.
(5) Vavilov, V. S. *J. Ph s. Chem. Solids* **1** , *8*, 223.
(6) Christensen, O. *J. Appl. Ph s.* **1 2**, *47*, 689.
(7) Shah, J. *Solid-State Electron.* **1** , *21*, 43.
(8) Shabaev, A.; Efros, A. L.; Nozik, A. J. *Nano Lett.* **200** , *6*, 2856